INS/GPS Integration: Global Observability Analysis

Yonggang Tang, Yuanxin Wu, Meiping Wu, Wenqi Wu, Xiaoping Hu, and Lincheng Shen

***Abstract*—Observability is an important aspect of the state-estimation problem in the integration of the inertial navigation system (INS) and the Global Positioning System (GPS) as it determines the existence and nature of solutions. In most previous research, conservative observability concepts, e.g., local observability and linear observability, have extensively been used to locally characterize the estimability properties. In this paper, a novel approach that directly starts from the basic observability definition is used to investigate the global observability of the nonlinear INS/GPS system with consideration of the lever arm uncertainty. A sufficient condition for the global observability of the system is presented. Covariance simulations with an extended Kalman filter (EKF) and a field test are performed to confirm the theoretical results. The global observability analysis approach is not only straightforward and comprehensive but also provides us with new insights that were unreachable by conventional methods.**

***Index Terms*—Global observability, inertial navigation system/Global Positioning System (INS/GPS), land vehicle, lever arm, linear observability.**

I. Introduction

MANY LAND vehicles are equipped with GPS receivers that can constantly provide information about the vehicle's position and velocity with pretty high accuracy, e.g., the accuracy of the carrier-phase differential GPS is at the centimeter level [1]. The main drawbacks of GPS are the following: 1) The satellite signals can be jammed; and 2) the outputs are at a relatively low rate (< 20 Hz). In contrast, the inertial navigation system (INS) is self-contained and has the ability to provide navigation solutions at a high rate, which is typically 100 Hz. The main disadvantage of an unaided INS system is an unbounded growth in the position and velocity errors. Due to their complementary attributes, the INS/GPS integration results in reliability, latency, bandwidth, and update rate improvements relative to the GPS-only approach [1].

In practice, a filter for recursive state estimation is often employed to correct the system errors using GPS aiding information. In designing the filter, the observability analysis is necessary because observability determines the existence of solutions and sets a lower limit on the estimation error [2], [3]. For an unobservable system, we cannot achieve successful estimation, even if the measurement is accurate enough. The observability of an INS/GPS integrated system has extensively been studied in many works [3]–[12]. Since there is no formal criterion available to examine the observability of a general nonlinear system, the linear observability analysis was usually investigated using the corresponding linearized models. For a linearized time-invariant system, the observability analysis is straightforward by testing the rank of the observability matrix [4], whereas the linearization is generally an implicit time-varying linear system [13], of which the analysis is cumbersome and involves the evaluation of the observability Grammian [14]. A control-theoretic approach was proposed in [3] and [7] to simplify the analysis. In this approach, the linear time-varying system was approximated by a piecewise constant model, and in each constant segment, a simplified null space test was performed to determine the observability properties. A general linear time-varying model was used in [5] to investigate the observability properties of INS/GPS errors. It was found that acceleration changes improve the observability of attitude and gyro bias, and attitude changes enhance the estimate of the lever arm. The theoretical result was supported by simulations and experiments [6]. However, no analytical observability conditions for general linear time-varying systems were obtained.

It should be noted that the aforementioned works were carried out based on the corresponding linearized model of the system. The linearization implies that the observability can only locally characterize the properties of the original nonlinear system [13], e.g., local observability [2], [15], [16] and linear observability [4], [8], [17]. These local concepts are identical to the (global) observability under investigation for a linear system but different for a nonlinear system. The local concepts are stronger than the global concepts for a nonlinear case in that a locally observable system is sure to be globally observable, but a globally observable system may locally be unobservable [15], [17]. The local concepts deal with the ability to distinguish the states from their neighbors in a small time interval or instantaneously, whereas the global concept describes the ability to estimate the states in the whole time span [15]. In other words, the requirements for global observability can more easily be met than the requirements for local observability. A global observability analysis can provide us with comprehensive instructions on whether the estimation is feasible under a given condition, as well as how to achieve the state estimate, e.g., by resorting to vehicle maneuvers.

Most recent works on the observability of nonlinear systems are based on the differential geometry and the Lie brackets [15]. However, the results derived are mainly theoretical and are still

Manuscript received April 25, 2007; revised September 14, 2007, February 26, 2008, and April 22, 2008. First published May 28, 2008; current version published March 17, 2009. This work was supported in part by the National Natural Science Foundation of China under Grant 60604011 and in part by the Research Fund for the Doctoral Program of Higher Education of China under Grant 20069998009. The review of this paper was coordinated by Dr. X. Wang.

Y. Tang is with the Air Force Academy, Guilin 541003, China (e-mail: tygbox@hotmail.com).

Y. Wu, M. Wu, and W. Wu are with the Department of Automatic Control, National University of Defense Technology, Changsha 410073, China (e-mail: yuanx_wu@hotmail.com).

X. Hu and L. Shen are with the College of Mechatronics and Automation, National University of Defense Technology, Changsha 410073, China.

Digital Object Identifier 10.1109/TVT.2008.926213

far away from a unified approach to check the observability in engineering applications [18], [19]. It is noted that the differential geometry or the Lie bracket is not the only solution of nonlinear observability analysis. In fact, most of the recent advances in dynamical system theory have been made by exploiting the structure inherent in special classes of systems [19]. To the authors' knowledge, there are still no works investigating the global observability of the nonlinear INS/GPS system. In this paper, we dwell on the analysis of the global observability of a nonlinear INS/GPS system with consideration of the lever arm uncertainty, directly starting from the observability definition.

For high-precision INS/GPS systems, the lever arm uncertainty acts as a major error source [20]. Large lever arm errors will decay the estimating precision of the position, velocity, attitude, and inertial sensor bias [20], [21]. As the INS is usually installed inside the vehicle, and the GPS antenna is mounted on the roof, it is difficult to directly measure the lever arm precisely. Instead, the lever arm could be considered as a state to be estimated in the filter [20], [22]. In this paper, a sufficient condition for estimating the lever arm, navigational parameters, and sensor bias is presented. It shows that the analysis is more straightforward, and the condition is looser, i.e., easier to be satisfied, than that obtained by previous linear analysis. Covariance simulations with an extended Kalman filter (EKF) and a field test are performed to support the theoretic results. It is shown that the global observability analysis is not only straightforward and intuitive but is also able to unveil more intrinsic relations between state observability and maneuvers than ever.

This paper is organized as follows. Section II briefly discusses the nonlinear dynamic model of the INS/GPS system. Section III is devoted to a rigorous global observability analysis. Simulations with an EKF are reported in Section IV. The results of a field test are presented in Section V. Discussions and conclusions are made in Section VI.

II. Nonlinear Dynamic Model

Since the GPS measurements are usually given in WGS-84, the Earth-centered Earth-fixed (ECEF) frame denoted by e-frame is taken as the navigation reference frame for convenience. The body frame is denoted by b-frame with the axes pointing forward, up, and right, respectively; the inertial frame is denoted by i-frame; the Earth-fixed tangential frame is denoted by t-frame; and the body-fixed local level frame is denoted by n-frame with the axes pointing to north, up, and east, respectively. The dynamic equations for a strapdown INS are given by [23]

$$\dot{p}^e = v^e \tag{1}$$

$$\dot{v}^e = C_b^e(f^b - \nabla) - 2\omega_{ie}^e \times v^e + g^e \tag{2}$$

$$\dot{C}_b^e = C_b^e\left(\omega_{eb}^b\times\right)$$

$$\omega_{eb}^b = \omega_{ib}^b - \varepsilon - C_e^b\omega_{ie}^e \tag{3}$$

where p^e and v^e are the INS's position and ground velocity in the e-frame, C_b^e is the body attitude matrix with respect to the e-frame, f^b is the specific force measured by accelerometers expressed in the b-frame, ∇ is the accelerometer bias, ω_{ie}^e is the Earth's rotation rate expressed in the e-frame, g^e is the gravity vector in the e-frame, ω_{eb}^b is the body angular rate with respect to the e-frame and expressed in the b-frame, $(\omega_{eb}^b\times)$ is the skew-symmetric matrix of ω_{eb}^b, and ε is the gyro drift. The gyro drift ε and the accelerometer bias ∇ are taken as random constants for simplicity, i.e.,

$$\dot{\varepsilon} = 0$$

$$\dot{\nabla} = 0. \tag{4}$$

There are mainly three types of INS/GPS integration, namely, loosely coupled integration, tightly coupled integration, and deeply coupled integration. Because there in no essential difference among them in the properties of observability if not considering the error states in GPS measurements, only the loosely coupled integration is considered hereafter for demonstration. Supposing that the vehicle is equipped with a single-antenna GPS receiver, the position measurement can be described as

$$y = p^e + C_b^e l^b \tag{5}$$

where l^b is the lever arm vector, which is a constant quantity, i.e.,

$$\dot{l}^b = 0. \tag{6}$$

III. Global Observability Analysis

Equations (1)–(3) are nonlinear, and there is no formal criterion available for such a system. Here, we study the global observability of the system directly from the observability definition.

The observability definition goes as follows [14].

Definition 1: A system is said to be observable if for any unknown initial state $x(t_0)$ there exists a finite $t_1 > t_0$ such that the knowledge of the input and output over $[t_0, t_1]$ suffices to uniquely determine the initial state $x(t_0)$. Otherwise, the system is said to be unobservable.

For the INS/GPS system under investigation, the states to be estimated comprise the position, velocity, attitude, lever arm, gyro drift, and accelerometer bias. The knowledge available includes the specific force measured by accelerometers, the body angular rate measured by gyros, and the position measured by the GPS receiver. According to the definition, if the initial states can uniquely be solved given the measurements in a finite-time interval, then the system is proved to be observable. Before proceeding, it is assumed that the vehicle runs near the Earth's surface with low speed so that the following relations hold: $\omega_{eb}^b \simeq \omega_{nb}^b \simeq \omega_{tb}^b$ [5]. A lemma necessary in the analysis is given below.

Lemma 1 [24]: For any two linearly independent vectors, if their coordinates in two arbitrary frames are given, then the attitude matrix between the two frames can uniquely be determined.

A. Case 1: Calibrated INS

For a calibrated high-precision INS, the sensor biases are well compensated, and only small quantities are left, e.g., less than $0.01^\circ/h$ for gyro drift and 10^{-5} g for accelerometer bias. Assuming that the update rate of measurements is 1 Hz, and the length of the lever arm is 10 m, the velocity errors induced by the gyro drift and the accelerometer bias in one update cycle are on the order of 10^{-7} m/s and 10^{-4} m/s, respectively, which are much lower than the GPS measurement noise. In this situation, negligence of the INS sensor biases has a little influence on the estimation of the lever arm and other states [10], [25], [26]. This statement will also be confirmed in Sections IV and V.

Letting $\varepsilon = \nabla = 0$, (1)–(3) are, respectively, reduced to

$$\dot{p}^e = v^e \tag{7}$$

$$\dot{v}^e = C_b^e f^b - 2\omega_{ie}^e \times v^e + g^e \tag{8}$$

$$\dot{C}_b^e = C_b^e \left(\omega_{eb}^b \times\right)$$

$$\omega_{eb}^b = \omega_{ib}^b - C_e^b \omega_{ie}^e. \tag{9}$$

Taking the derivative on both sides of (5) and using (7), we have

$$\dot{y} = v^e + \dot{C}_b^e l^b. \tag{10}$$

Supposing that the vehicle runs along a straight line, the body attitude does not change, i.e., $\dot{C}_b^e = 0$. We have

$$\dot{y} = v^e. \tag{11}$$

Taking derivative again on both sides of (11) and using (8) yields

$$\ddot{y} = C_b^e f^b - 2\omega_{ie}^e \times \dot{y} + g^e. \tag{12}$$

Let

$$z = \ddot{y} + 2\omega_{ie}^e \times \dot{y} - g^e. \tag{13}$$

Designate the inertial frame as the e-frame at the initial time t_0. The relationship between the body attitude matrix C_b^e and the initial body attitude matrix $C_b^e(t_0)$ can be described as

$$C_b^e = C_i^e C_b^e(t_0) C_b^{b(0)} \tag{14}$$

where $b(0)$ denotes the b-frame at t_0. Substituting (13) and (14) into (12) yields

$$z = C_i^e C_b^e(t_0) C_b^{b(0)} f^b. \tag{15}$$

Multiplying C_e^i on both sides and reorganizing the terms, we have

$$C_b^e(t_0) C_b^{b(0)} f^b = C_e^i z. \tag{16}$$

Since the matrix C_e^i is a function of the Earth rotation rate ω_{ie}^e, and the position is directly measured so that the gravity vector g^e is known (the errors due to unknown lever arm is negligible), the items on the right side are known. Denoting $C_b^{b(0)} f^b$ by $f^{b(0)}(t)$, $f^{b(0)}(t)$ is the measured specific force expressed in the initial body frame $b(t_0)$. Noting that $C_b^{b(0)}$ and f^b can be computed from the outputs of gyroscopes and measured by accelerometers, respectively, $f^{b(0)}(t)$ is known. According to Lemma 1, the initial attitude matrix $C_b^e(t_0)$ can uniquely be determined on the condition that there exist two linearly independent $f^{b(0)}(t_1)$ and $f^{b(0)}(t_2)$ for $t_1 \neq t_2$, which is not difficult to satisfy for a vehicle running with a time-varying velocity.

As for a vehicle with constant velocity, we have

$$\ddot{y} = 0.$$

We rewrite (16) as

$$C_b^{b(0)} f^b = C_e^b(t_0) C_e^i \left(2\omega_{ie}^e \times \dot{y} - g^e\right). \tag{17}$$

If there exist two linearly independent $C_e^i(2\omega_{ie}^e \times \dot{y} - g^e)$, then $C_b^e(t_0)$ can uniquely be determined. Because the value of $2\omega_{ie}^e \times \dot{y}$ is much smaller than g^e, the linear independency mainly depends on $C_e^i g^e$. Noting that $C_e^i g^e$ is the gravity expressed in the inertial frame, of which the direction changes with the Earth rotation, $C_e^i g^e(t_1)$ and $C_e^i g^e(t_2)$ are linearly independent for any time $t_1 \neq t_2$ (within 24 h), and as a result, the matrix $C_b^e(t_0)$ can uniquely be determined. Hence, if there is a path segment with $\dot{C}_b^e = 0$, the attitude is observable, and the body attitude matrix at any time is known using (14).

The differential equation of the velocity in the i-frame is

$$\dot{v}^i = C_b^i f^b + C_e^i \left(g^e + \omega_{ie}^e \times (\omega_{ie}^e \times p^e)\right). \tag{18}$$

The relationship between v^e and v^i can be formulated as

$$v^i = C_e^i \left(\omega_{ie}^e \times p^e + v^e\right). \tag{19}$$

On the path segment with $\dot{C}_b^e = 0$, using (18) and (19) can be rewritten as

$$C_e^i \left(\omega_{ie}^e \times p^e + \dot{y}\right) = v^i(t_0) + \int_{t_0}^{t} \left[C_b^i f^b + C_e^i \left(g^e + \omega_{ie}^e \times (\omega_{ie}^e \times p^e)\right)\right] d\tau \tag{20}$$

where

$$C_e^i \left(\omega_{ie}^e \times p^e + \dot{y}\right) \int_{t_0}^{t} \left[C_b^i f^b + C_e^i \left(g^e + \omega_{ie}^e \times (\omega_{ie}^e \times p^e)\right)\right] d\tau$$

are known, and then $v^i(t_0)$ can be determined. Since the inertial frame is defined as the e-frame at t_0, using (19), we have

$$v^e(t_0) = v^i(t_0) - \omega_{ie}^e \times p^e(t_0) \tag{21}$$

and as a result, $v^e(t_0)$ can uniquely be determined. Hereby, the velocity is observable, and the velocity at any time is known.

Suppose that there is a path segment with a variant attitude, i.e., $\dot{C}_b^e \neq 0$. Substituting (9) into (10) yields

$$\dot{y} = v^e + C_b^e \left(\omega_{eb}^b \times\right) l^b. \tag{22}$$

The terms $\dot{y}$, v^e, and $C_b^e(\omega_{eb}^b\times) = C_b^e(\omega_{ib}^b\times) - (\omega_{ie}^e\times)C_b^e$ are already known. Noticing that the rank of $C_b^e(\omega_{eb}^b\times)$ is 2, we know that if there exist two path segments with $\dot{C}_b^e \neq 0$ on which the body angular rate with respect to the e-frame ω_{eb}^b is linearly independent, the lever arm l^b can be uniquely determined, i.e., the lever arm is observable.

Since C_b^e and l^b are known, using (5), p^e at any time can be determined, i.e., the position is observable.

The foregoing results are summarized by the following theorem.

Theorem 1: For a calibrated high-precision INS/GPS, if the vehicle runs along a trajectory on which there are

1) one path segment where $\dot{C}_b^e = 0$;
2) two path segments where $\omega_{eb}^b \neq 0$, and ω_{eb}^b is linearly independent on these two segments;

then the body attitude, velocity, position, and lever arm are observable.

Remark 1: The sufficient condition is moderate, which means that the requirements can be met in almost any practical running trajectory. The first condition requires the vehicle to hold a constant attitude, which is easily satisfied when the vehicle goes straight on a flat road. The second condition needs the direction of ω_{eb}^b to vary in running. It can be fulfilled if the vehicle turns with its body lurching for centripetence, or there exist both turning and pitching in the running.

Remark 2: Theorem 1 only gives a sufficient condition in that the system may be observable under other situations.

Remark 3: From (16), we can conclude that the more linearly independent $f^{b(0)}(t)$ is, the more easily can the initial attitude matrix be determined. The same story lies between ω_{eb}^b and the lever arm. In other words, the degree of linear independency of $f^{b(0)}(t)$ determines the degree of attitude observability, and the degree of linear independency of ω_{eb}^b determines the degree of lever arm observability. This finding is generally consistent with previous works [3], [5], stating that the variation of f^b improves the estimation of attitude, and the variation of ω_{eb}^b enhances the estimability of the lever arm.

Remark 4: There is no requirement for the linear acceleration to make the attitude observable, which is in contrast with the linear observability conditions in [3] and [5]. This is due to the absence of gyro drift and accelerometer bias. We see that the attitude is globally observable, even when the vehicle is stationary or running with constant velocity, which explains the principle of self-alignment on a stationary base using a high-precision INS. In the low-cost INS case in a subsequent section, the attitude would be unobservable in a constant-velocity constant-attitude situation due to the large sensor bias [9], and maneuvers would be needed to render it observable [7].

Remark 5: By a similar analysis, we can infer that all the states, except for the position, would be observable when the velocity acted as the measurements.

B. Case 2: Uncalibrated INS

In this case, the INS sensors are assumed to be not precisely calibrated, or a low-cost inertial measurement unit is used. The gyro bias and the accelerometer bias are significant and must be taken into consideration.

Supposing that the vehicle runs along a straight line on the ground, and the body attitude does not change, taking the derivative on both sides of (11) and using (2) yield

$$\ddot{y} = C_b^e(f^b - \nabla) - 2\omega_{ie}^e \times \dot{y} + g^e. \tag{23}$$

Taking derivative again on both sides yields

$$C_b^e \dot{f}^b = \dddot{y} + 2\omega_{ie}^e \times \ddot{y} + \dot{g}^e. \tag{24}$$

The items on the right side are already known. If there are two linear independent $\dot{f}^b$, then the attitude matrix C_b^e on this segment can be determined. Since all the terms in (23) except ∇ are known, ∇ can uniquely be determined. As the attitude does not change, we have $\omega_{eb}^b = 0$. Using (3), ε can be determined as

$$\varepsilon = \omega_{ib}^b - C_e^b \omega_{ie}^e. \tag{25}$$

Hereby, the gyro drift ε and the accelerometer bias ∇ are observable.

Now that ε and ∇ are known. Following the calibrated case, the other states can be proved to be observable. The results are summarized as the second theorem.

Theorem 2: For an uncalibrated INS/GPS, if the vehicle runs along a trajectory on which there are

1) one path segment that $\dot{C}_b^e = 0$, and there are two linearly independent $\dot{f}^b$ on this segment;
2) two path segments that $\omega_{eb}^b \neq 0$, and ω_{eb}^b is linearly independent on these two segments;

then the body attitude, velocity, position, gyro drift, accelerometer bias, and lever arm are all observable.

Remark 6: The first condition requires that the direction of $\dot{f}^b$ should change on a straight path segment $(\dot{C}_b^e = 0)$. For a land vehicle, it can be fulfilled at the instantaneous moment that the vehicle begins to turn after running along a straight line with varying acceleration. Since this moment is instantaneous, we predict that the observability of ε and ∇ is relatively weak and that this type of maneuver needs to be repetitiously operated to achieve a satisfactory estimation.

Remark 7: On the straight segment $(\dot{C}_b^e = 0)$, taking the derivative on both sides of (24), we have

$$C_b^e \ddot{f}^b = \left(\dddot{y} + 2\Omega_{ie}^e \ddot{y} - \dot{g}^e\right)'. \tag{26}$$

It shows that two linear independent $\ddot{f}^b$ can also make ε and ∇ observable. By repeating this procedure, it can be proved that if there are two linear independent k-order derivatives $(k \geq 1)$, ε and ∇ are observable. In contrast to [5, Property 3.6] (see Appendix), the condition in Theorem 2 is more general and more practical than that of a linear observability. As an example, suppose that the vehicle runs along a straight line with varying acceleration and "jumps" at times with constant attitude. In this situation, f^b and its derivatives $\dot{f}^b, \ldots, \overset{(k)}{f^b}$ stay in the vertical plane that is parallel to the vehicle's driving force vector, and any three vectors in $f^b, \dot{f}^b, \ldots, \overset{(k)}{f^b}$ are linearly dependent. Hence, the condition in [5, Property 3.6] cannot be

sufficient, and we can say nothing about their linear observability. The conservativeness will be highlighted in the next section.

Remark 8: In Theorems 1 and 2, the *existence* of a path segment $\dot{C}_b^e = 0$ is required. Under the assumptions of low speed that we have made before, this requirement is easy to be met for vehicles that run on the ground or water surface. Therefore, it can be argued that Theorems 1 and 2 are more applicable for low-speed vehicles in practice.

IV. Simulations and Results

It is well known that an unobservable state cannot be estimated, even in the most favorable situations [3], [5]. If a state can be estimated, then it is valid to be observed. To support the theoretical results, some typical motions of vehicle on a designed trajectory are simulated, and an extended Kalman filter (EKF) is used to estimate the states. Both the calibrated and uncalibrated INS cases are considered. To illustrate the difference between Theorem 2 and [5, Property 3.6], a "jump" case is fabricated.

The update rate of the INS is 100 Hz, and the navigation solution is corrected by the EKF using position measurements from a single-antenna GPS receiver at the rate of 1 Hz. The lever arm between the INS and the antenna is set to $[1 \quad 1 \quad 1]^{\mathrm{T}}$ in meters in the b-frame, and the initial attitude errors of roll, yaw, and pitch are supposed to be 5°, 10°, and 5°. All the noises are assumed to be Gaussian white. The standard deviations (STD) of the differential global positioning system position measurement noise are $[0.06 \quad 0.08 \quad 0.06]^{\mathrm{T}}$ in meters [5].

A. Case 1: Calibrated INS

In this simulation, the drift rate of the gyroscope and the bias of the accelerometer are set to be $0.005^\circ/h$ and 5×10^{-5} g, respectively. We design a closed trajectory consisting of four straight segments and four curve segments. In the first 10 s, the vehicle stands still. Then, it accelerates for 20 s, keeps a constant velocity for 5 s, and decelerates for 20 s. Between 55 and 60 s, the vehicle climbs up and down, then goes straight for 5 s, and turns right with its body lurching for 5 s. This process is repeated to form a closed path. The kinematics of the vehicle is shown in Figs. 1–5.

The gyro drift and the accelerometer bias are ignored in the filter. The estimation errors of the attitude are shown in Fig. 6. The scaled errors in 60–100 s are shown as dashed lines in the right panel for a detailed view, with the thick labels on the right side of the panel. As shown, the errors in the roll and pitch quickly decrease for they could directly be determined by measuring the gravity vector. The yaw error drifts in the first 10 s when the vehicle keeps stationary and begins to decrease at 10 s when the vehicle starts accelerating. At 100 s, all three angular errors are very close to zero (see dashed lines). The relationship between drive acceleration and specific force is shown in Fig. 7. It shows that the specific force becomes linearly independent when the magnitude of acceleration varies to enhance the observability of attitude.

In Fig. 8, the lever arm errors are plotted. The errors significantly decrease after the vehicle passes two curve segments

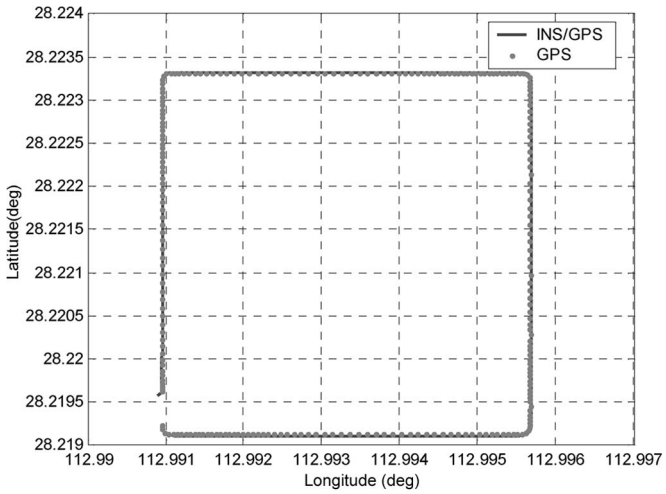

Fig. 1. Trajectory of the vehicle.

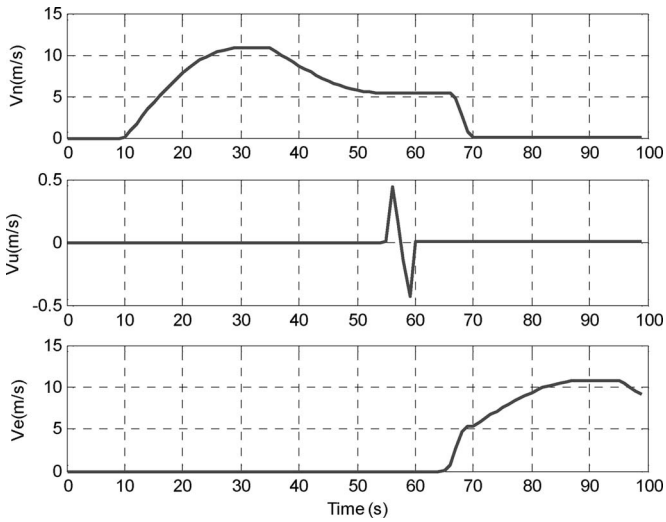

Fig. 2. Velocity of the vehicle in case 1.

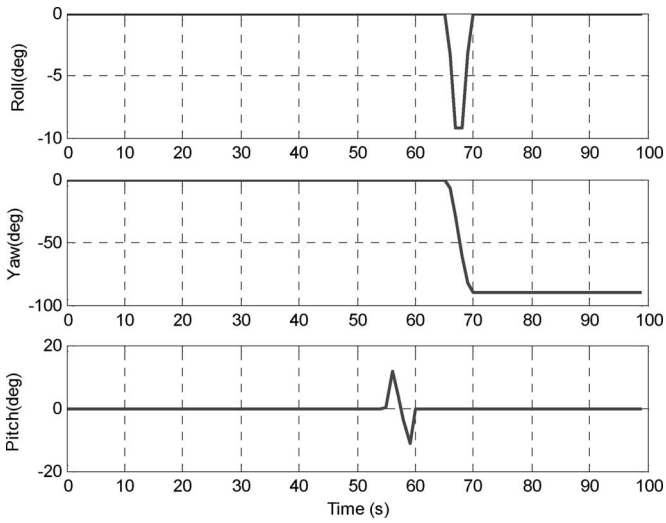

Fig. 3. Attitude of the vehicle in case 1.

in 55–60 and 65–70 s, respectively. As shown in Fig. 9, in 65–70 s, the vehicle's body lurches with turning due to the suspending system and tires. The direction of the angular rate

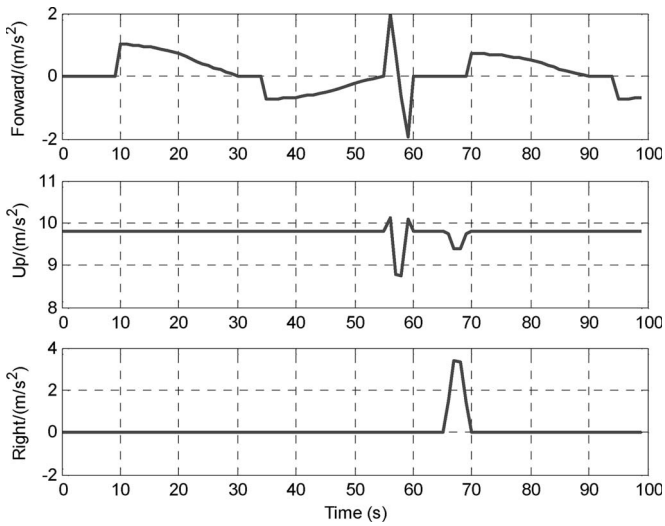

Fig. 4. Specific force in case 1.

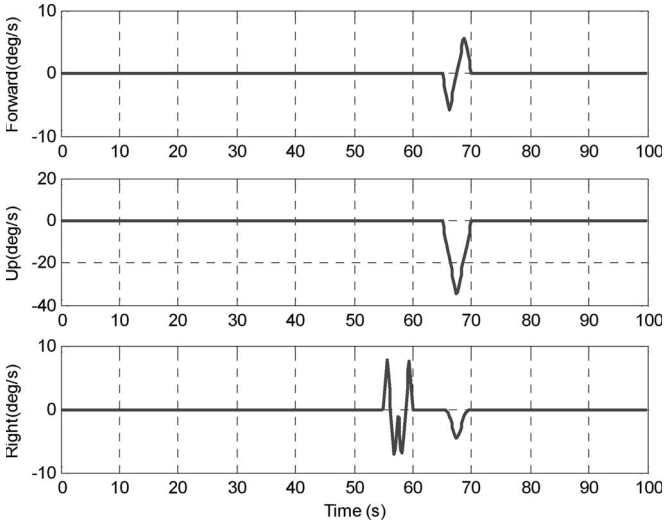

Fig. 5. Angular rate of the vehicle in case 1.

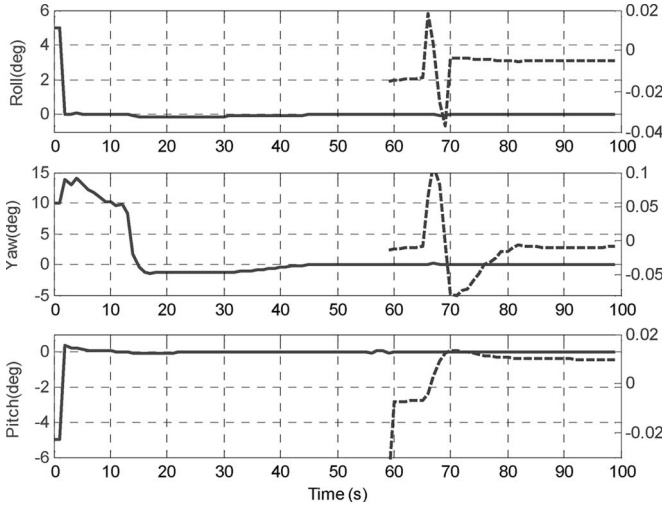

Fig. 6. Attitude errors in case 1 (scaled errors in 60–100 s are given in the right panel).

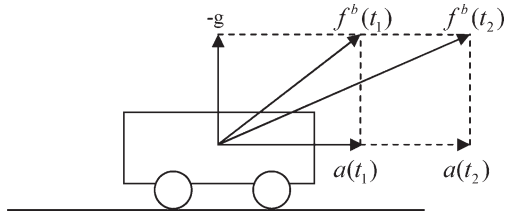

Fig. 7. Drive acceleration and linearly independent specific force on the straight path segment. $a(t)$ is the acceleration caused by the composition of drive force and friction force, g is the acceleration of gravity, and $f^b(t)$ is the specific force.

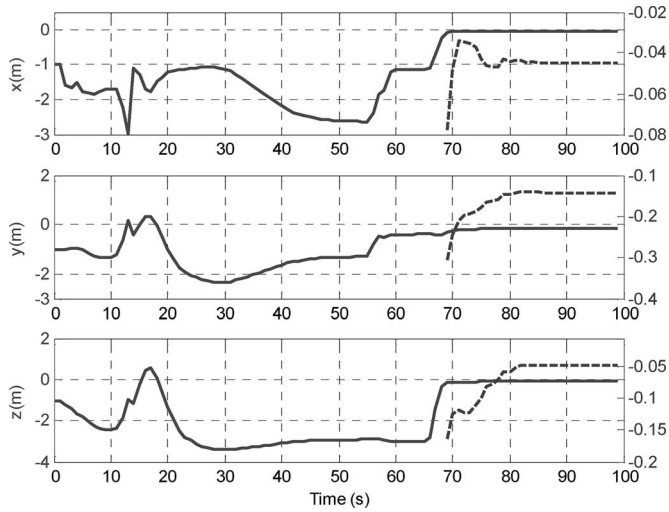

Fig. 8. Lever arm errors in case 1 (scaled errors in 70–100 s are given in the right panel).

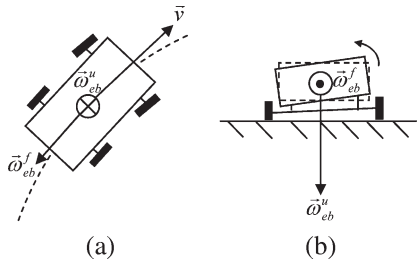

Fig. 9. Example of a linearly independent body angular rate in the b-frame on a curve segment. (a) Top view. (b) Back view. $\vec{\omega}^u_{eb}$ is the body angular rate in the up direction, $\vec{\omega}^f_{eb}$ is the body angular rate in the forward direction, and $\vec{v}$ is the ground velocity.

in b-frame varies with the tilt, which renders the lever arm observable. In 55–60 s, the lever arm errors in the z-direction almost do not change, and we observed in many simulations that the lever arm errors in the other two directions may not decrease until the start of turning, which shows that a single-degree angular motion like that in 55–60 s is not enough for the lever arm to be observable. It is noted that the lever arm errors in the up direction more slowly decreases (see dashed lines). Referring to Fig. 5, we can find that the yaw angle changes more sharply than the roll and pitch angles so that the linear independency of ω^b_{eb} in the up direction is greater than that in the other two directions. As a result, the degree of the lever arm's observability in two horizontal directions is

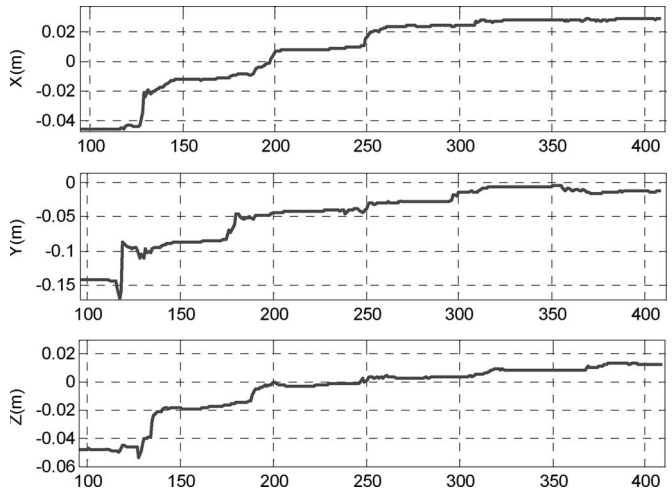

Fig. 10. Lever arm errors in 100–400 s in case 1.

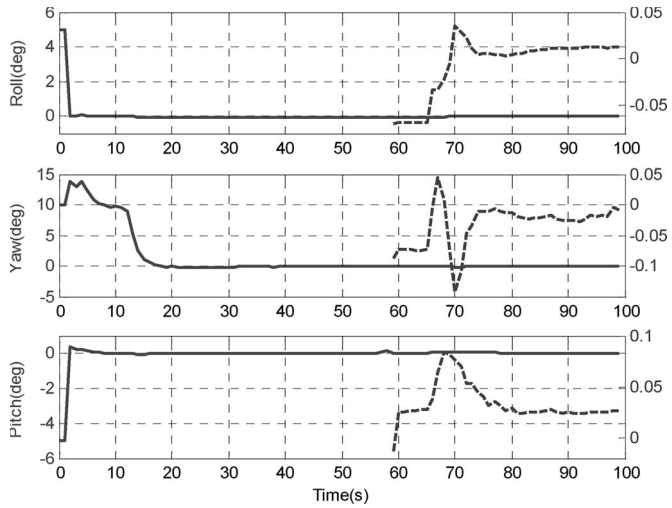

Fig. 11. Attitude errors when augmented with the gyro drift and the accelerometer bias in case 1 (scaled errors in 60–100 s are given on the right sides of the panels).

larger than that in the up direction (as shown in Remark 3). In Fig. 10, the lever arm errors in 100–400 s are shown. The errors approach nonzero steady values, which are mostly owed to the modeling errors, after the vehicle passes more curve segments. At 400 s, the values are 0.03, -0.01, and -0.02 m, respectively, which shows that the iterative angular motions are in favor of achieving a satisfactory accuracy.

For comparison, the filter augmented with gyro drift and accelerometer bias is considered. The results of the lever arm and attitude estimation are shown in Figs. 11 and 12. Comparatively, there are no substantial differences in the results.

B. Case 2: Uncalibrated INS

The drift rate of the gyroscope and the bias of the accelerometer are set to be $0.05^\circ/\text{s}$ and 0.05 m/s^2, respectively. The error state vector is composed of position, velocity, attitude, lever arm, gyro drift, and accelerometer bias. The trajectory is slightly different from case 1 in canceling the pitch changes.

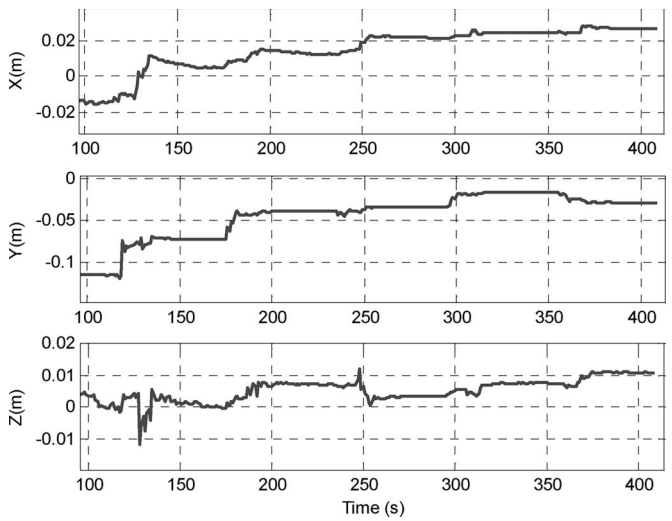

Fig. 12. Lever arm errors when augmented with the gyro drift and the accelerometer bias in case 1.

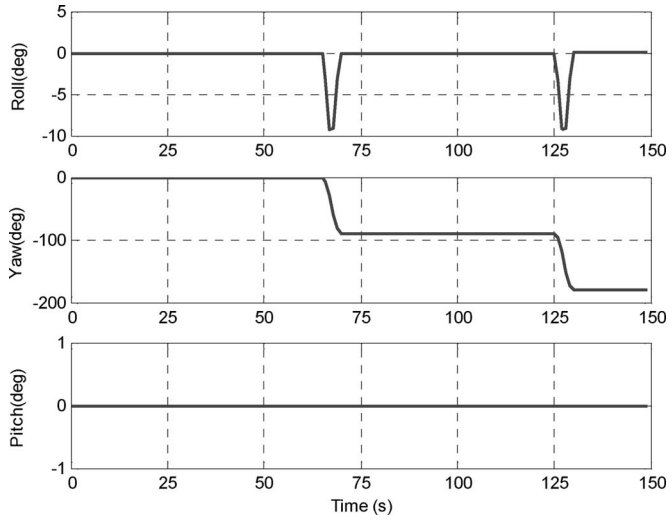

Fig. 13. Attitude of the vehicle in case 2.

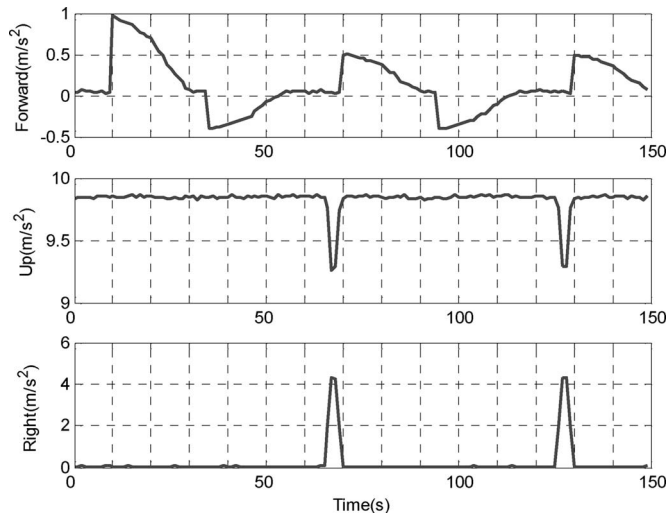

Fig. 14. Specific force in case 2.

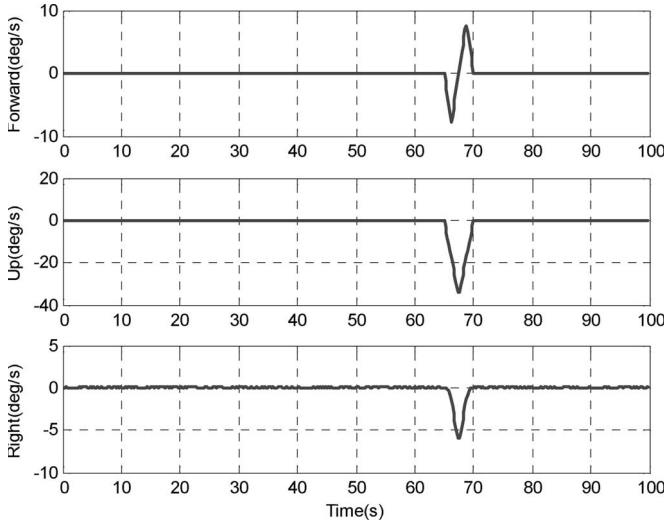

Fig. 15. Angular rate in case 2.

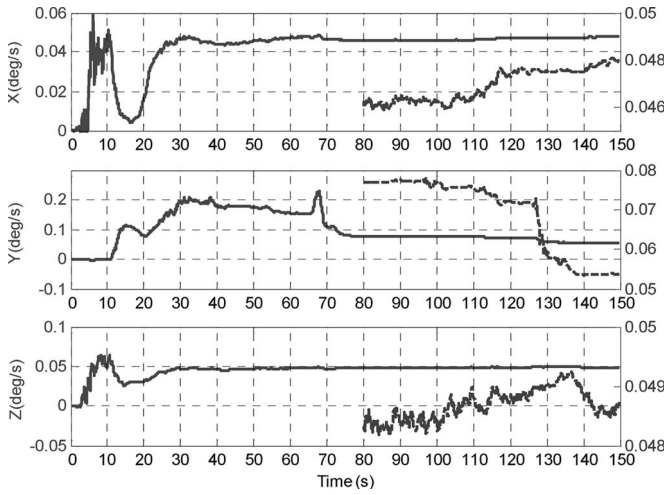

Fig. 16. Estimation of the gyro drift rate in case 2 (scaled errors in 80–100 s are given on the right sides of the panels).

The vehicle's attitude, specific force, and angular rate are shown in Figs. 13–15.

In Figs. 16 and 17, the estimated gyro drift and accelerometer bias converge toward their true value, respectively, after 70 s. Until 150 s, the estimated values have come very close to the truth (see dashed lines). The standard deviations of the estimation errors are plotted in Figs. 18 and 19. The standard deviation of the gyro drift errors in the up direction and that of the accelerometer bias in the forward and right directions are evidently reduced when the vehicle turns in 65–70 s. At the begin-to-turn moment, the direction of f^b sharply changed so that $\dot{f}^b$ is linearly independent on this path segment. The attitude errors and lever arm errors are shown in Figs. 20 and 21, respectively. The attitude errors are remarkably reduced when the vehicle accelerates since 70 s before which the sensor bias has been estimated. Although there are no changes in the pitch angle, the lever arm errors are still evidently reduced during 65–70 s. Referring to Fig. 15, we can find that the angular rate changes in all three directions in time, which is sufficient for the

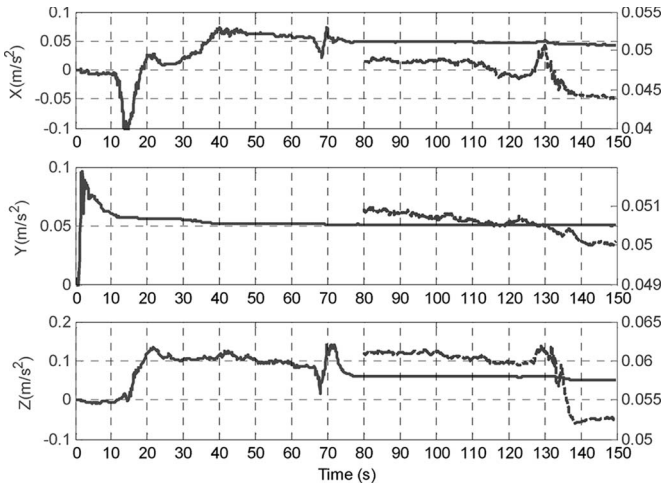

Fig. 17. Estimation of the accelerometer bias in case 2 (scaled errors in 80–100 s are given in the right panel).

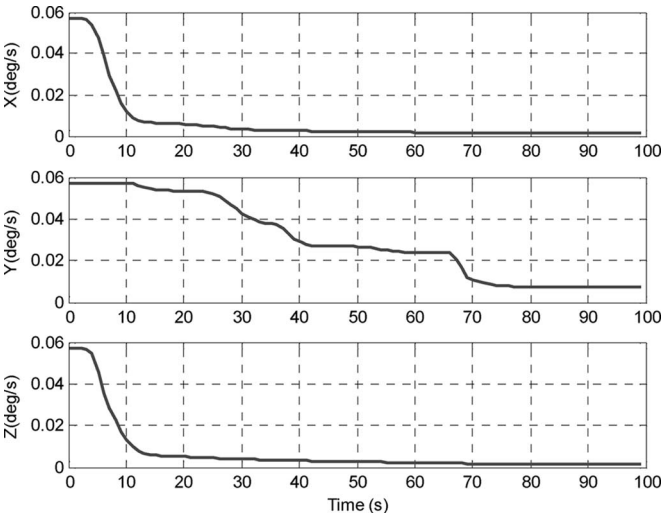

Fig. 18. Standard deviation of the gyro drift rate estimation error in case 2.

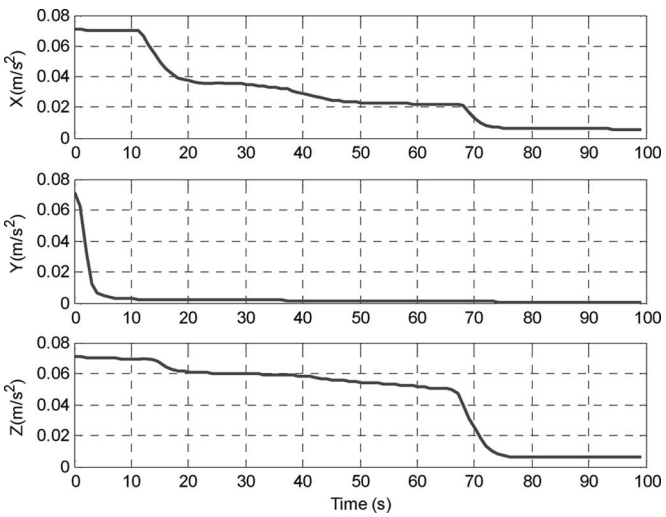

Fig. 19. Standard deviation of the accelerometer bias estimation error in case 2.

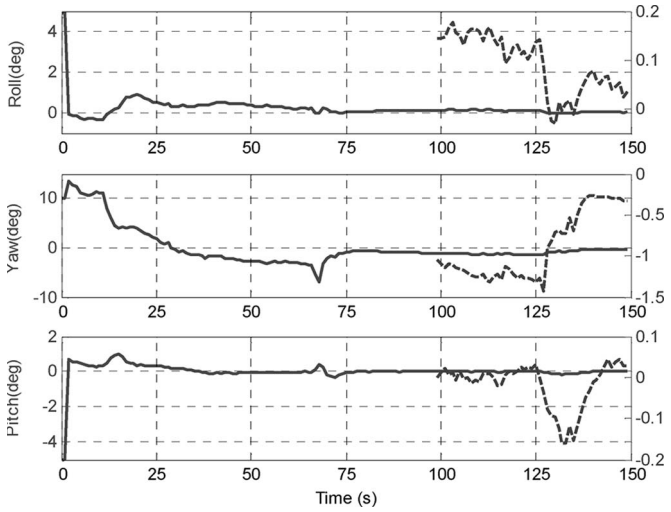

Fig. 20. Attitude errors in case 2 (scaled errors in 100–150 s are given on the right sides of the panels).

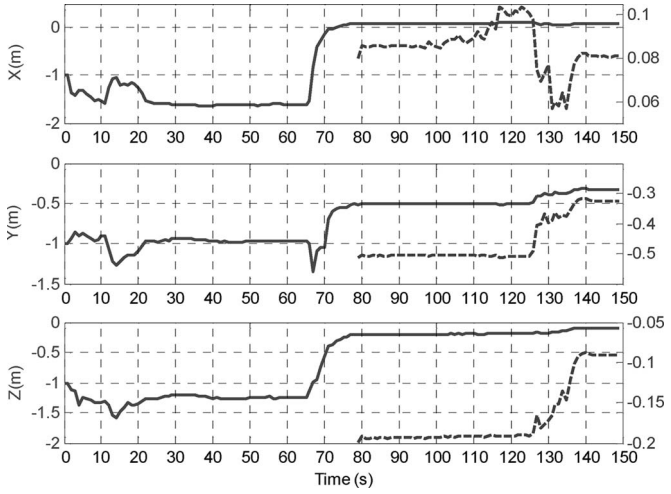

Fig. 21. Lever arm errors in case 2 (scaled errors in 80–150 s are given on the right sides of the panels).

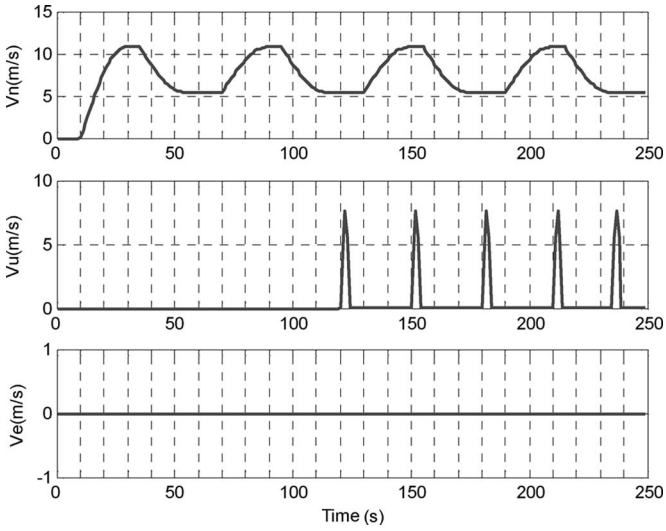

Fig. 22. Velocity in the jump case (case 3).

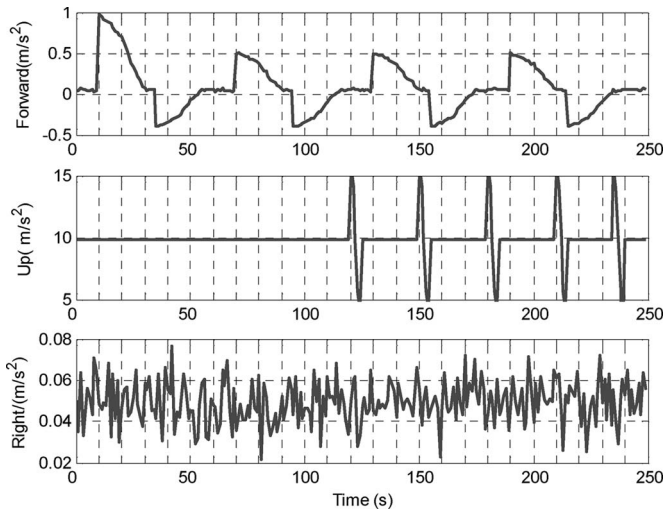

Fig. 23. Specific force in the jump case (case 3).

requirements for the lever arm to be observable. Affected by the big sensor bias, the accuracies of the attitude and lever arm are much lower than those in case 1. It will take more maneuvering to achieve a satisfying accuracy.

C. Case 3: Jump

According to Theorem 2, the gyro drift and the accelerometer bias are observable if $\dot{f}^b$'s are linearly independent on the path segment without angular movement. A path is fabricated here to verify this conclusion. The vehicle runs along a straight line with varying acceleration and begins to jump vertically once every 30 s without changing the attitude after 120 s. The velocity and specific force are shown in Figs. 22 and 23. In straight-line running, $\dot{f}^b$ lies along the forward direction in the b-frame. When the vehicle jumps, f^b vertically changes so that $\dot{f}^b$ becomes linearly independent on the path segment, and as a result, all states except the lever arm should be observable.

The estimation results are shown in Figs. 24–26. In Fig. 24, the yaw errors are reduced with the vehicle's acceleration since 10 s. The errors in the roll and pitch are remarkably reduced from the beginning and are further reduced after 120 s when the accelerometer bias is estimated. In Fig. 25, the gyro drift estimation flows at the beginning due to the big attitude errors and gradually converges to its true value with the reduction of attitude errors. Fig. 26 shows that the estimation of accelerometer bias starts to converge stepwise along with the jump motion. As a comparison, the estimation of accelerometer bias without jumping, i.e., there is only acceleration along the forward direction, is shown in Fig. 27. The accelerometer bias slowly converges in the x-direction and comes to a false value in the z-direction. The simulation results show that a linearly independent $\dot{f}^b$ is sufficient for the attitude and the sensor bias to be observable. This fact is in accord with Theorem 2 but conflicts with [5, Property 3.6].

V. Field-Test Results

A field test is performed to estimate the lever arm. A ring laser strapdown INS and a single-antenna OEM4 GPS receiver

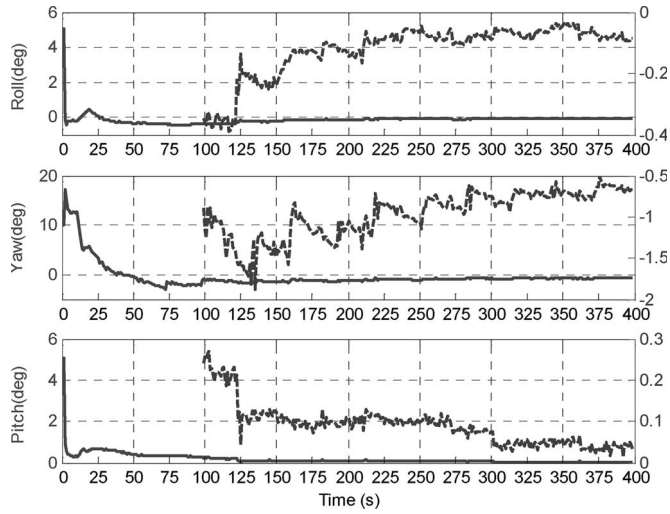

Fig. 24. Attitude errors in the jump case (case 3, scaled errors in 100–400 s are given on the right sides of the panels).

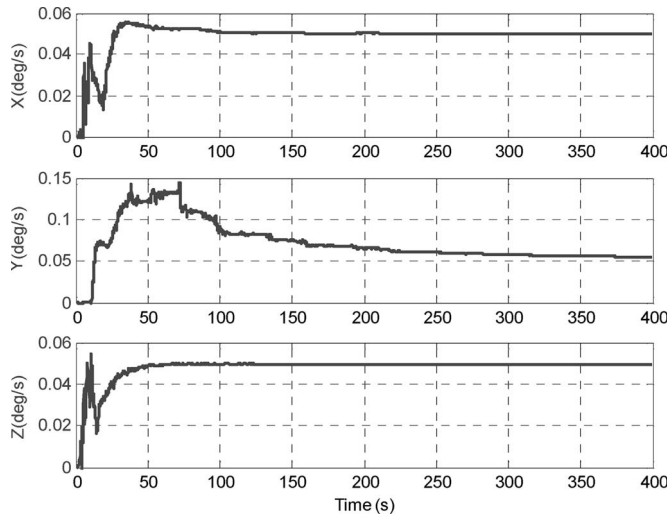

Fig. 25. Estimation of gyro drift in the jump case (case 3).

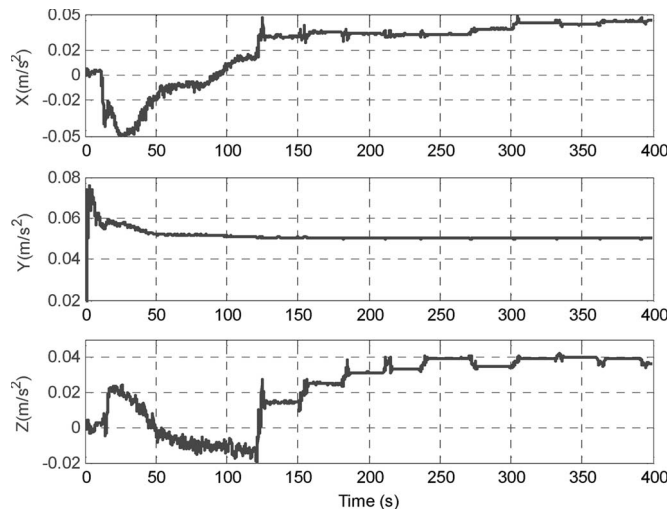

Fig. 26. Estimation of accelerometer bias in the jump case (case 3).

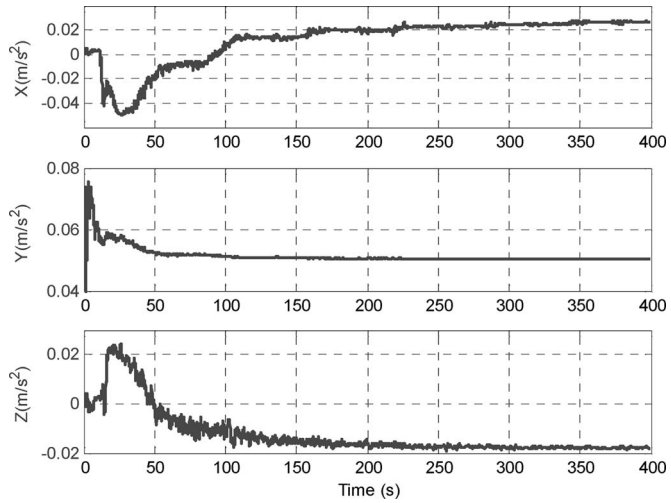

Fig. 27. Estimation of accelerometer bias without jump (case 3).

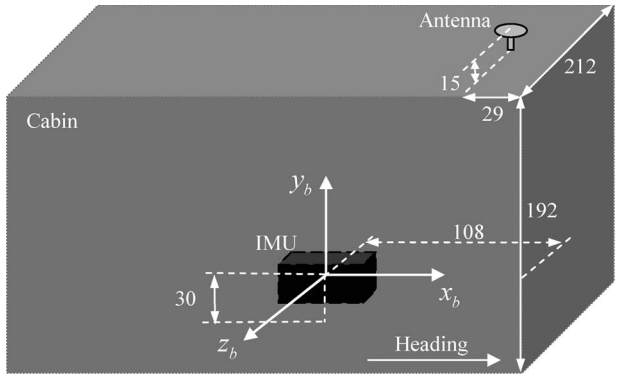

Fig. 28. Location of sensors and definition of the body frame in the field test (length in centimeters).

augmented by Omnistar (SBAS, Satellite-Based Augmentation System) are used in the test. The stabilities of the gyro drift rate and accelerometer bias are $0.01^\circ/h$ (1σ) and 5×10^{-5} g(1σ), respectively. The update rate of the INS is 50 Hz. The GPS receiver provides position measurements at the rate of 1 Hz with an accuracy higher than 1 m (1σ) most of the time (occasionally the signal from Omnistar is masked). An EKF is applied to estimate the lever arm and navigation errors.

The INS is installed inside the cabin of a van, and the antenna is mounted on the roof. The location of the sensors and the definition of the body frame are shown as Fig. 28. The quantities are manually measured as an approximate reference for the evaluation of the estimates. The lever arm is coarsely

$$l_x^b = 1.08 \text{ m} - 0.29 \text{ m} = 0.79 \text{ cm}$$

$$l_y^b = 1.92 \text{ m} + 0.15 \text{ m} - 0.30 \text{ m} = 1.77 \text{ m}$$

$$l_z^b = 0 \text{ m}.$$

During the test, the vehicle runs along a rectangle-shaped trajectory in the campus, as in Fig. 29. The velocity, attitude,

Fig. 29. Trajectory (red thick line) of field test (captured from Google Earth).

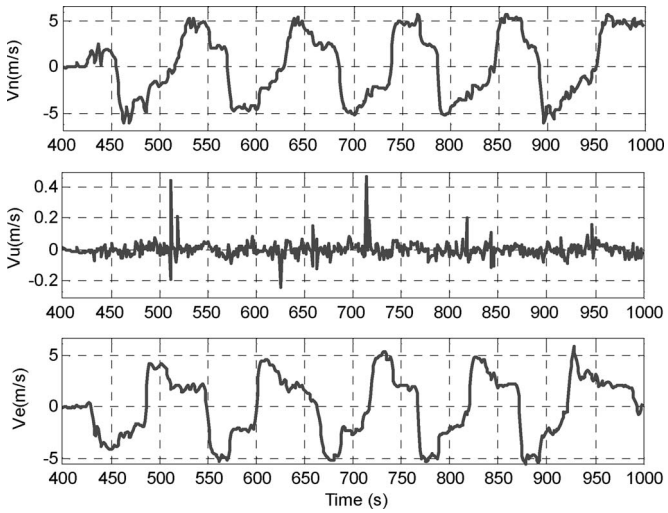

Fig. 30. Velocity of the vehicle in the field test.

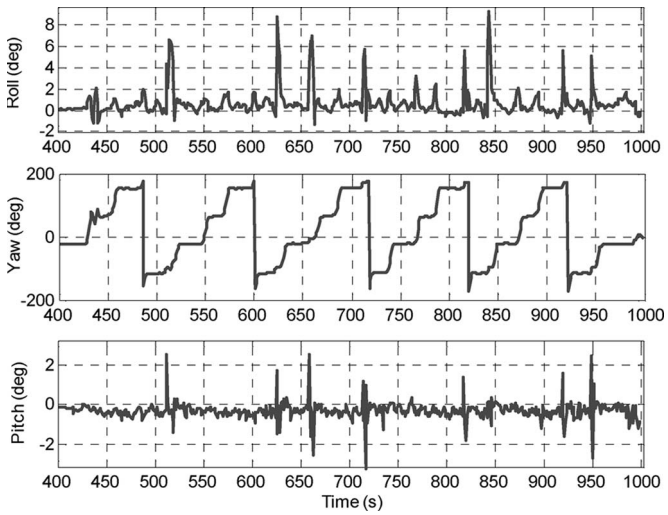

Fig. 31. Attitude of the vehicle in the field test.

specific force, and angular rate of the vehicle are plotted in Figs. 30–33, respectively. As shown in these figures, the vehicle begins to move at 400 s and made an "S"-shape movement in

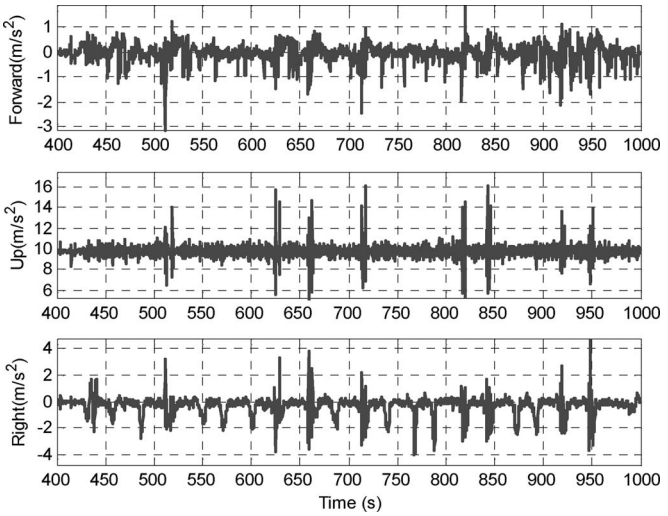

Fig. 32. Specific force in the field test.

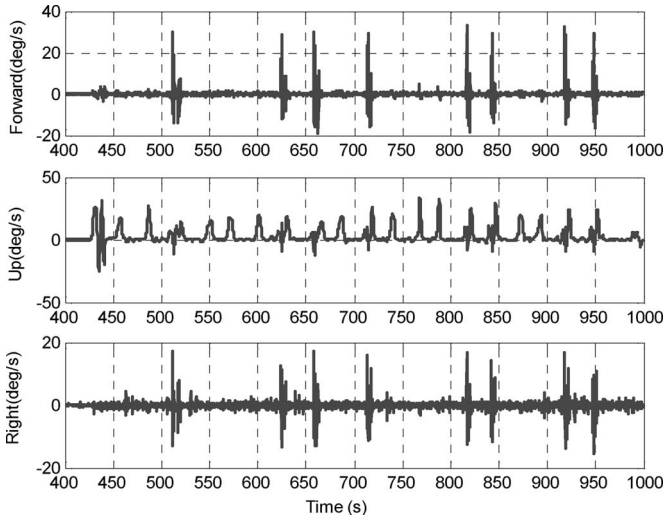

Fig. 33. Angular rate of the vehicle in the field test.

420–450 s. In each round, the vehicle accelerates and decelerates on straight segments and turns at the corners with its body tilting.

The estimation of the lever arm gradually stabilizes with the vehicle's motion, which is plotted in Fig. 34. Until 1000 s, the lever arm has converged to near 0.77 m in x, 1.74 m in y, and 0.06 m in z. The values are very close to the approximate reference. The estimated lever arm in 420–450 s is shown in Fig. 35, i.e., when the estimation begins to converge. The trajectory and angular rates in this span are plotted in Figs. 36 and 37, respectively. It is shown that when the vehicle conducts an "S"-shape motion, the angular rate varies from $-25^\circ/\mathrm{s}$ to $25^\circ/\mathrm{s}$ in the up direction and $-3^\circ/\mathrm{s}$ to $4^\circ/\mathrm{s}$ in the forward direction, respectively, which satisfies the sufficient condition for the lever arm's observability in Theorem 1. As shown in Fig. 35, the estimated lever arm quickly changes from its initial value to the stable value. See the scaled lever arm estimation on the right panel of Fig. 34 (dashed lines). The ranges of variation in the last 100 s are 0.76–0.78, 1.65–1.8, and 0.04–0.08 m in

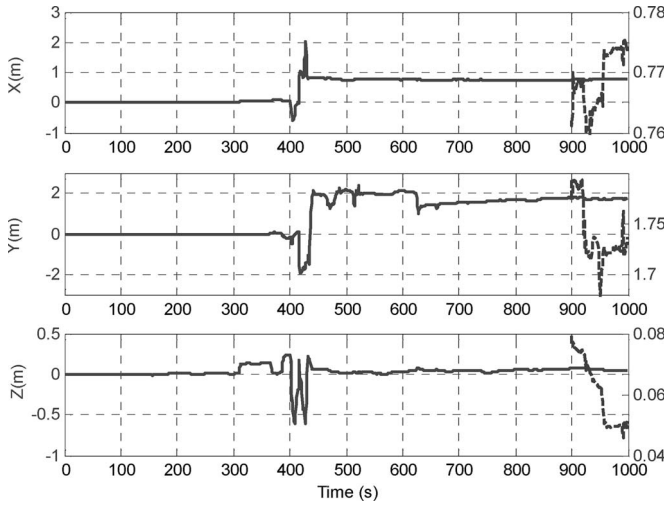

Fig. 34. Estimation of the lever arm in the field test.

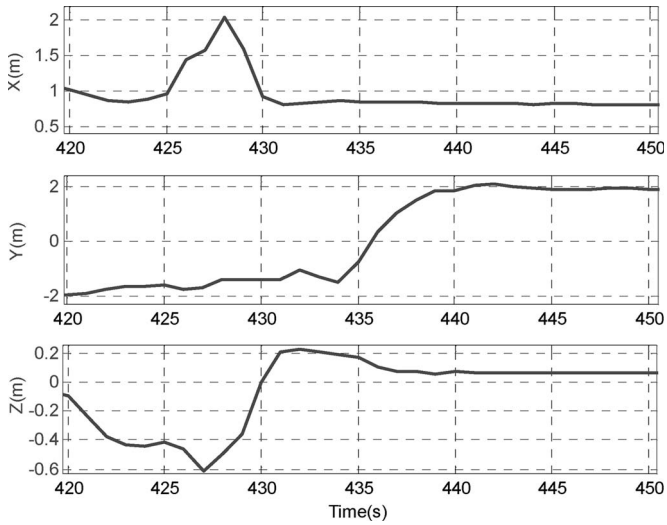

Fig. 35. Estimated lever arm in 420–450 s.

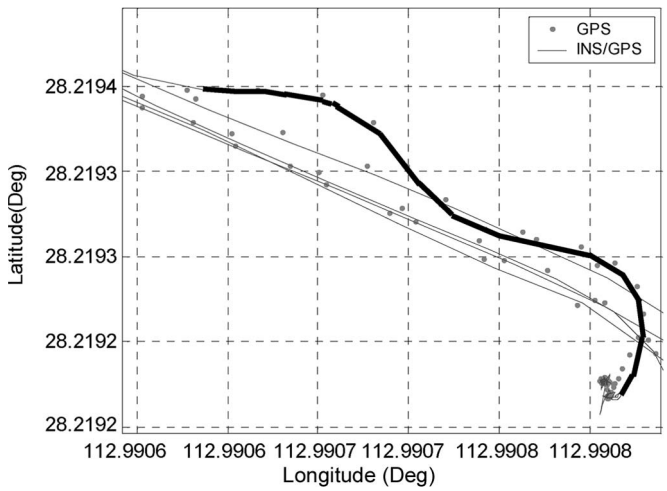

Fig. 36. Trajectory in 420–450 s (dark thick line).

x, y, and z, respectively. Therefore, the estimation accuracy is inferred to be at the centimeter level in the horizontal directions and at the decimeter level in the up direction.

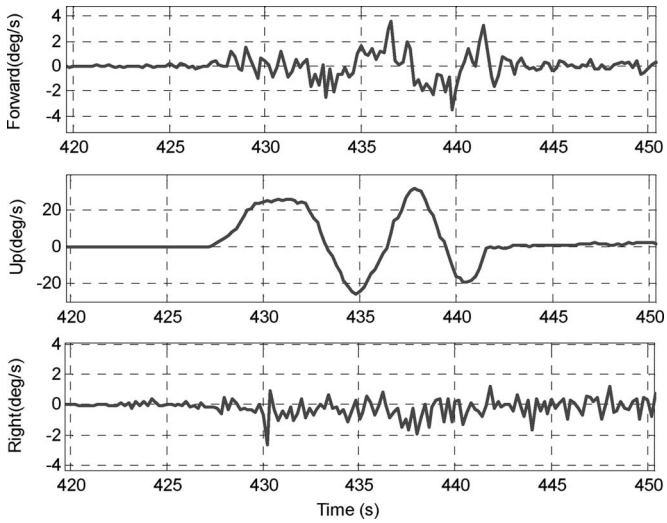

Fig. 37. Angular rate in 420–450 s.

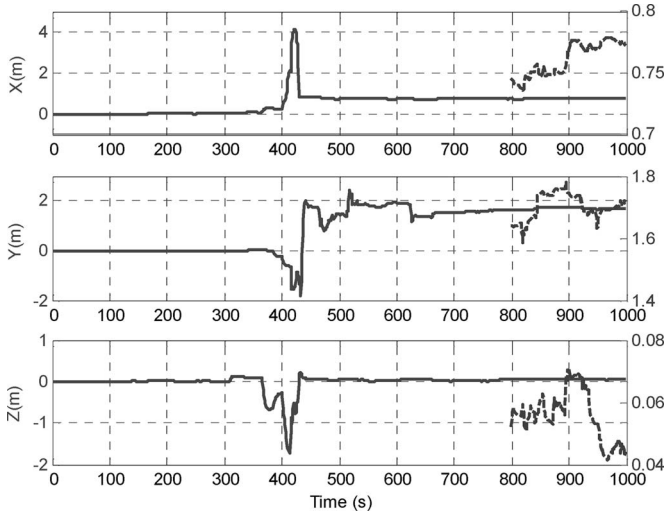

Fig. 38. Estimation of the lever arm augmented with gyro drift and accelerometer bias in the field test.

For comparison, the filter augmented with the gyro drift and the accelerometer bias is considered. The result of the lever arm is shown in Fig. 38, which shows no substantial differences because the INS system used highly accurate.

VI. Discussions and Conclusion

The main contribution of this paper is applying the global observability analysis approach to the specific problem of the INS/GPS integration system, in which we more comprehensively and profoundly reveal the relationship between the system observability and the vehicle movements in a simple and intuitive manner. A sufficient condition for the global observability of position, velocity, attitude, gyro/accelerometer bias, and lever arm is presented. The condition is explicit, analytic, and easier to satisfy compared with previous works [5], [6], [20], [22].

Analysis, simulations, and field testing have lead to the following conclusions.

1) We have established a sufficient requirement on the vehicle motion for global observability by Theorems 1 and 2. The result is generally in agreement with the linear observability analysis in previous works [5], [7]. It is asserted that translatory motions, i.e., acceleration changes, can enhance the observability of the attitude and sensor bias, and angular motions can enhance the observability of the lever arm [5]. This conclusion is further clarified here by showing that the observability of the attitude rests with the linear independency of the specific force expressed in an inertial frame, i.e., $f^{b(0)}(t)$. The observability of the sensor bias is associated with the linear independency of the time derivatives of a specific force, i.e., $\dot{f}^b$. The observability of the lever arm depends on the linear independency of the body angular rate ω_{eb}^b.
2) The motion requirements of global observability are easier to meet than that of linear observability, e.g., a linearly independent $\dot{f}^b$ is sufficient to render the attitude and sensor bias observable, whereas the requirement for any three of the vectors $f^b, \dot{f}^b, \ddot{f}^b, \ldots, f^{b(k)}$ to be linearly independent [5] is too conservative. In the fabricated jump case, the states are observable in the global sense but not in the linear sense, which convincingly shows the overpessimism of the local observability concept.
3) The sufficient conditions for global observability are applicable for a general time-varying system. In contrast, by linear observability analysis, the development is nontrivial, and the analytic condition is difficult to acquire for time-varying systems.
4) For a well-calibrated, high-precision INS/GPS system, the effect of a sensor bias on the estimation of the lever arm can be neglected.

Because the observability analysis is performed based on a general land INS/GPS system model, the insights thus obtained are, of course, valid on any vehicular INS/GPS application. Additionally, it is not a difficult job to extend the analysis to related applications.

APPENDIX
PROPERTY 3.6 [5]

Suppose that R_b^e is a constant, and f^b is time varying. If any three vectors in $f^b, \dot{f}^b, \ddot{f}^b, \ldots, f^{b(n-3)}$ are linearly independent, then the system (A, C) has three unobservable modes δl. Otherwise, (A, C) has at least one additional unobservable mode. (The symbol meanings follow [5].)

ACKNOWLEDGMENT

The authors would like to thank H. Mu, L. Lu, J. Lian, and X. He for the helpful discussions on a couple of related topics.

REFERENCES

[1] J. A. Farrell, T. D. Givargis, and M. J. Barth, "Real-time differential carrier phase GPS-aided INS," *IEEE Trans. Control Syst. Technol.*, vol. 8, no. 4, pp. 709–721, Jul. 2000.
[2] S. Wijesoma, K. W. Lee, and J. I. Guzman, "On the observability of path constrained vehicle localisation," in *Proc. IEEE Intell. Transp. Syst. Conf.*, Toronto, ON, Canada, 2006, pp. 1513–1518.
[3] D. Goshen-Meskin and I. Y. Bar-Itzhack, "Observability analysis of piecewise constant systems—Part I: Theory," *IEEE Trans. Aerosp. Electron. Syst.*, vol. 28, no. 4, pp. 1056–1067, Oct. 1992.
[4] J. H. Dambeck, "Observability and controllability analysis for a strapdown inertial navigation system," in *Proc. 3rd Int. High Precision Navigat.*, Bonn, Germany, 1995.
[5] S. Hong, M. H. Lee, H.-H. Chun, S.-H. Kwon, and J. L. Speyer, "Observability of error states in GPS/INS integration," *IEEE Trans. Veh. Technol.*, vol. 54, no. 2, pp. 731–743, Mar. 2005.
[6] S. Hong, M. H. Lee, H.-H. Chun, S.-H. Kwon, and J. L. Speyer, "Experimental study on the estimation of lever arm in GPS/INS," *IEEE Trans. Veh. Technol.*, vol. 55, no. 2, pp. 431–448, Mar. 2006.
[7] D. Goshen-Meskin and I. Y. Bar-Itzhack, "Observability analysis of piecewise constant systems—Part II: Application to inertial navigation in-flight alignment," *IEEE Trans. Aerosp. Electron. Syst.*, vol. 28, no. 4, pp. 1068–1075, Oct. 1992.
[8] I. Rhee, M. F. Abdel-Hafez, and J. L. Speyer, "On the observability of an integrated GPS/INS during maneuvers," in *Proc. ION GPS*, Portland, OR, 2002.
[9] Y. F. Jiang and Y. P. Lin, "Error estimation of INS ground alignment through observability analysis," *IEEE Trans. Aerosp. Electron. Syst.*, vol. 28, no. 1, pp. 92–97, Jan. 1992.
[10] I. Y. Bar-Itzhack and B. Porat, "Azimuth observability enhancement during inertial navigation system in-flight alignment," *J. Guid. Control Dyn.*, vol. 3, no. 4, pp. 337–344, 1980.
[11] I. Y. Bar-Itzhack and N. Bermant, "Control theoretic approach to inertial navigation systems," *J. Guid. Control Dyn.*, vol. 11, no. 3, pp. 237–245, 1988.
[12] J. G. Park, J. G. Lee, J. Kim, and C. G. Park, "Observability analysis of SDINS/GPS in-flight alignment," in *Proc. ION GPS*, Salt Lake City, UT, 2000.
[13] W. J. Terrell, "Local observability of nonlinear differential-algebraic equations (DAEs) from the linearization along a trajectory," *IEEE Trans. Autom. Control*, vol. 46, no. 12, pp. 1947–1950, Dec. 2001.
[14] C.-T. Chen, *Linear System Theory and Design*, 3rd ed. New York: Holt, Rinehart, and Winston, 1999.
[15] R. Hermann and A. J. Krener, "Nonlinear controllability and observability," *IEEE Trans. Autom. Control*, vol. AC-22, no. 5, pp. 728–740, Oct. 1977.
[16] Z. Chen, K. Jiang, and J. C. Hung, "Local observability matrix and its application to observability analyses," in *Proc. 16th Annu. Conf. IEEE Ind. Electron. Soc.*, 1990, pp. 100–103.
[17] H. G. Kwatny and B.-C. Chang, "Symbolic computing of nonlinear observable and observer forms," *Appl. Math. Comput.*, vol. 171, no. 2, pp. 1058–1080, 2005.
[18] M. W. Hirsch, "The dynamical systems approach to differential equations," *Bull. (New Ser.) Amer. Math. Soc.*, vol. 11, no. 1, pp. 1–64, 1984.
[19] J. L. Casti, "Recent developments and future perspectives in nonlinear system theory," *SIAM Rev.*, vol. 24, no. 3, pp. 301–331, Jul. 1982.
[20] S. Hong, Y.-S. Chang, S.-K. Ha, and M.-H. Lee, "Estimation of alignment errors in GPS/INS integration," in *Proc. ION GPS*, Portland, OR, 2002.
[21] J. Seo, J. G. Lee, and C. G. Park, "Leverarm compensation for integrated navigation system of land vehicles," in *Proc. IEEE Conf. Control Appl.*, Toronto, ON, Canada, 2005, pp. 523–528.
[22] S. Hong, M. H. Lee, S. H. Kwon, and H. H. Chun, "A car test for the estimation of GPS/INS alignment errors," *IEEE Trans. Intell. Transp. Syst.*, vol. 5, no. 3, pp. 208–218, Sep. 2004.
[23] M. Wei and K. P. Schwarz, "A strapdown inertial algorithm using an Earth-fixed Cartesian frame," *J. Inst. Navigat.*, vol. 37, no. 2, pp. 153–167, 1990.
[24] H. D. Black, "A passive system for determining the attitude of a satellite," *AIAA J.*, vol. 2, no. 7, pp. 1350–1351, Jul. 1964.
[25] I. Y. Bar-Itzhack, "Minimal order time sharing filters for INS in-flight alignment," *J. Guid. Control Dyn.*, vol. 5, pp. 396–402, 1982.
[26] X. He, Y. Chen, and H. B. Iz, "A reduced-order model for integrated GPS/INS," *IEEE Aerosp. Electron. Syst. Mag.*, vol. 13, no. 3, pp. 40–45, Mar. 1998.

Yonggang Tang received the B.Sc. and M.Sc. degrees in automatic control and the Ph.D. degree from the National University of Defense Technology, Changsha, China, in 1994, 2001, and 2008, respectively.

He is currently a Lecturer with the Air Force Academy, Guilin, China. His current research interests include navigation systems, general estimation theory, information fusion, and C^4ISRT systems.

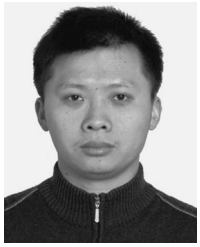

Yuanxin Wu was born in Jinan, China, in 1976. He received the B.Sc. and Ph.D. degrees from the National University of Defense Technology, Changsha, China, in 1998 and 2005, respectively.

Since 2005, he has been with the National University of Defense Technology, where he was a Lecturer from 2005 to 2007 and is currently an Assistant Professor. His current research interests include navigation systems, general estimation theory, statistical signal processing, and the application of Clifford algebra in engineering.

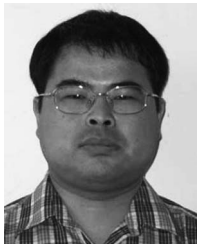

Meiping Wu was born in Fujian, China, in 1971. He received the B.Sc. and M.Sc. degrees in aviation mechanics and the Ph.D. degree in navigation, guidance, and control from the National University of Defense Technology, Changsha, China, in 1993, 1996, and 2000, respectively.

He is currently an Associate Professor and an Associate Director with the Department of Automatic Control, National University of Defense Technology. He is an expert of the 863 High Technology Project. His scientific interests include aircraft navigation, guidance, and control.

Wenqi Wu was born in Nei Monggu, China, in 1967. He received the B.Sc. degree in automation from Tianjin University, Tianjin, China, in 1988 and the M.Sc. and Ph.D. degrees in navigation, guidance, and control from the National University of Defense Technology, Changsha, China, in 1991 and 2002, respectively.

From August 2007 to February 2008, he was a Visiting Scholar with the Institute of Navigation, Stuttgart University, Stuttgart, Germany. He is currently a Professor with the Department of Automatic Control, National University of Defense Technology. His research interests include navigation, remote sensing, and automatic control.

Xiaoping Hu was born in Sichuan, China, in 1960. He received the B.Sc. and M.Sc. degrees in automatic control systems and aircraft designing from the National University of Defense Technology, Changsha, China, in 1982 and 1985, respectively.

He is currently a Professor and the Dean of the College of Mechatronics and Automation, National University of Defense Technology. His scientific interests include inertial and satellite navigation, aircraft guidance, and control.

Lincheng Shen was born in 1965. He received the B.S., M.S., and Ph.D. degrees from the National University of Defense Technology, Changsha, China, in 1986, 1990, and 1994, respectively.

He is currently a Full Professor in the field of control science and technology with the National University of Defense Technology. His research interests include mission planning and the control of unmanned aerial vehicles (UAVs), artificial intelligence (AI), and bionic robot control technology.